

SANDIA REPORT

SAND2000-0830
Unlimited Release
Printed April 2000

RECEIVED
JUN 08 2000
OSTI

Raman Study of Lead Zirconate Titanate Under Uniaxial Stress

D. R. Tallant, R. L. Simpson, J. M. Grazier, D. H. Zeuch, W. R. Olson, and B. A. Tuttle

Prepared by
Sandia National Laboratories
Albuquerque, New Mexico 87185 and Livermore, California 94550

Sandia is a multiprogram laboratory operated by Sandia Corporation,
a Lockheed Martin Company, for the United States Department of
Energy under Contract DE-AC04-94AL85000.

Approved for public release; further dissemination unlimited.



Sandia National Laboratories

Issued by Sandia National Laboratories, operated for the United States Department of Energy by Sandia Corporation.

NOTICE: This report was prepared as an account of work sponsored by an agency of the United States Government. Neither the United States Government, nor any agency thereof, nor any of their employees, nor any of their contractors, subcontractors, or their employees, make any warranty, express or implied, or assume any legal liability or responsibility for the accuracy, completeness, or usefulness of any information, apparatus, product, or process disclosed, or represent that its use would not infringe privately owned rights. Reference herein to any specific commercial product, process, or service by trade name, trademark, manufacturer, or otherwise, does not necessarily constitute or imply its endorsement, recommendation, or favoring by the United States Government, any agency thereof, or any of their contractors or subcontractors. The views and opinions expressed herein do not necessarily state or reflect those of the United States Government, any agency thereof, or any of their contractors.

Printed in the United States of America. This report has been reproduced directly from the best available copy.

Available to DOE and DOE contractors from
Office of Scientific and Technical Information
P.O. Box 62
Oak Ridge, TN 37831

Prices available from (703) 605-6000
Web site: <http://www.ntis.gov/ordering.htm>

Available to the public from
National Technical Information Service
U.S. Department of Commerce
5285 Port Royal Rd
Springfield, VA 22161



DISCLAIMER

**Portions of this document may be illegible
in electronic image products. Images are
produced from the best available original
document.**

**SAND2000-0830
Unlimited Release
Printed April 2000**

Raman Study of Lead Zirconate Titanate Under Uniaxial Stress

D. R. Tallant and R. L. Simpson
Materials Characterization Department

J. M. Grazier and D. H. Zeuch
Geomechanics Department

W. R. Olson and B. A. Tuttle
Electronic and Optical Materials Department

Sandia National Laboratories
P.O. Box 5800
Albuquerque, NM 87185-1411

Abstract

We have used micro-Raman spectroscopy to monitor the ferroelectric (FE) - to - antiferroelectric (AFE) phase transition in PZT ceramic bars during the application of uniaxial stress. We designed and constructed a simple loading device, which can apply sufficient uniaxial force to transform reasonably large ceramic bars while being small enough to fit on the mechanical stage of the microscope used for Raman analysis. Raman spectra of individual grains in ceramic PZT bars were obtained as the stress on the bar was increased in increments. At the same time gauges attached to the PZT bar recorded axial and lateral strains induced by the applied stress. The Raman spectra were used to calculate an "FE coordinate", which is related to the fraction of FE phase present. We present data showing changes in the FE coordinates of individual PZT grains and correlate these changes to stress-strain data, which plot the macroscopic evolution of the FE-to-AFE transformation. Our data indicates that the FE-to-AFE transformation does not occur simultaneously for all PZT grains but that grains react individually to local conditions.

Contents

Introduction	1
Experimental.....	2
Stress-Strain Data	8
Raman Spectra from AFE and FE Phases of PZT	15
Extraction of FE/AFE Phase Information from the Raman Spectra	16
Data from the PZT 98/2 Stress/Raman Experiment	18
Data from the PZT 4.4 Stress/Raman Experiments.....	19
Data from the PZT 4.7 Stress/Raman Experiments.....	24
Summary	30
Acknowledgements.....	31
References	32
Distribution.....	33

Figures

1 Schematic diagram of the stressed PZT/Raman spectroscopy experiment.....	4
2 Photograph of the spectrometer, microscope and load frame	4
3 Load frame with PZT bar/endcaps mounted	5
4 Micrograph of area of PZT 4.7 (SP14B #8)	8
5 Stress-strain data for SP-15A #11A, a bar of PZT 98/2	9
6 Stress-Strain data for SP12H-16 #12A, a bar of PZT 4.4.....	11
7 Stress-strain data for SP12H-16 #10, a bar of PZT 4.4.....	11
8 Stress-strain data for SP12H-16 #9, a bar of PZT 4.4.....	12
9 Stress-strain data for SP12H-16 #14, a bar of PZT 4.4.....	12
10 Stress-strain data for SP14B #2, a bar of PZT 4.7	13
11 Stress-strain data for SP14B #7, a bar of PZT 4.7	13
12 Stress-strain data for SP14B #8, a bar of PZT 4.7	14
13 Stress-strain data for SP14B #15, a bar of PZT 4.7	14
14 Raman spectra of the AFE and FE phases of reference PZT compositions	16
15 Raman spectra from location Deep #1 (PZT 4.7, SP14B #8).....	17
16 FE coordinates versus applied stress for a bar of AFE-phase PZT 98/2	18
17 FE coordinates versus applied stress for a bar of FE-phase PZT 4.4.....	20
18 FE coordinates versus applied stress for a bar of FE-phase PZT 4.4.....	21
19 FE coordinates versus applied stress for a bar of FE-phase PZT 4.4.....	22
20 FE coordinates versus applied stress for a bar of FE-phase PZT 4.4.....	23
21 FE coordinates versus applied stress for a bar of FE-phase PZT 4.7	26
22 FE coordinates versus applied stress for a bar of FE-phase PZT 4.7	27
23 FE coordinates versus applied stress for a bar of FE-phase PZT 4.7	28
24 FE coordinates versus applied stress for a bar of FE-phase PZT 4.7	29

Table

1 Stressed PZT Bars	3
---------------------------	---

Raman Study of Lead Zirconate Titanate Under Uniaxial Stress

Introduction

Lead zirconate titanate (PZT) ceramic materials are used in weapons applications because of their ferroelectric properties. $Pb_{0.99}Nb_{0.02}(Zr_{1-x}Ti_x)_{0.99}O_3$ with $x=0.05$ (PZT 95/5) is used in voltage bars in neutron generators, providing power when an explosively driven pressure wave depolarizes the voltage bar as a result of a ferroelectric (FE) to anti-ferroelectric (AFE) phase change. While there is a general knowledge of the conditions required to produce an FE-to-AFE phase change, detailed predictions of PZT 95/5 behavior as functions of composition, temperature, shear stress and microstructure are currently not possible. Understanding the microstructure dependence of the ferroelectric performance is a particular concern to the PZT Supply Team, which is developing a new process for producing PZT in-house to meet the on-going needs of the stockpile. Current efforts in modeling are seeking to predict phase behavior in dielectric solids, such as PZT 95/5. An improved understanding of the microstructural evolution of the FE-to-AFE transformation will aid the development of models which seek to predict phase behavior.

For PZT with the composition $Pb_{0.99}Nb_{0.02}(Zr_{1-x}Ti_x)_{0.99}O_3$, the FE phase has the rhombohedral crystal habit. Materials with $x = 4.3$ or greater have been determined to be in the FE phase at equilibrium. The AFE phase has the orthorhombic crystal habit and is the stable configuration at $x= 2.0$. The unit cell of the AFE phase is smaller than that of the FE phase. Compressing the unit cell with hydrostatic pressures of a few hundred MPa will effect the FE-to-AFE transformation.

Raman spectra of PZT materials containing tin (PZST) show distinctive differences when compositional variations result in FE/AFE phase changes [Tallant, 1996]. The Raman bands showing the greatest effect with phase change are low frequency modes ($50 - 200 \text{ cm}^{-1}$) believed to be associated with cation motion. The relatively high Raman efficiency of these materials greatly aids the ability to record low frequency Raman bands. A previous study [Tallant, 1997] indicated that Raman spectroscopy can detect pressure-induced FE-to-AFE phase changes in PZT materials. A PZT 95/5 (FE phase) material containing niobium was stressed to 600 MPa, a pressure that is sufficient to induce an FE-to-AFE phase transformation. The Raman spectrum of the stressed PZT was measured after release of the stress and compared to that of a sample of the same composition which had not been stressed. The Raman spectrum of the stressed material showed small, but distinctive differences consistent with the presence of a small amount of AFE phase. X-ray diffraction confirmed that a small (probably a few percent) amount of AFE phase remained in the previously stressed material.

Both Fritz [1979] and Zeuch *et al.* [1999] have shown that the FE-to-AFE transformation of unpoled PZT 95/5 ceramic can be triggered by uniaxial compression. The most recent results [Zeuch *et al.*, 1999] indicate that the transformation begins when the applied uniaxial stress reaches a value similar to that of the hydrostatic pressure for transformation. For PZT ceramic bars prepared using the "mixed-oxide"

process, this pressure or stress is in the approximate range of 200 to 250 MPa. A similar transformation pressure is assumed for the "PZT ceramic bars prepared by "Chem-Prep" techniques.

In this project we used micro-Raman spectroscopy to monitor the FE-to-AFE phase transition in microscopic crystals within PZT ceramic bars as a function of uniaxial stress. We designed and constructed a simple loading device, which can apply sufficient uniaxial force to transform reasonably large ceramic bars, while being small enough to fit on the mechanical stage of the microscope used for micro-Raman analysis. Raman spectra of individual grains in ceramic PZT bars were obtained as the stress on the bar was increased in increments. At the same time gauges attached to the PZT bar recorded axial and lateral strains induced by the applied stress. The Raman spectra were used to calculate an "FE coordinate", which is related to the fraction of FE phase present. We present data showing changes in the FE coordinates of individual PZT grains and correlate these changes to stress-strain data, which plot the macroscopic evolution of the FE-to-AFE transformation. Our data indicates that the FE-to-AFE transformation does not occur simultaneously for all PZT grains but that grains react individually to local conditions.

Experimental

Lead Zirconate Titanate (PZT) Materials

The material on which we performed stress experiments is unpoled, polycrystalline lead zirconate titanate with niobium (PZT), which has the general formula $Pb_{0.99}Nb_{0.02}(Zr_{1-x}Ti_x)_{0.98}O_3$. At the composition $x=0.02$ (PZT 98/2) the material is in an anti-ferroelectric (AFE) phase. Two compositions in the ferroelectric (FE) phase region were used in these experiments. One ferroelectric composition has $x = 0.044$ (PZT 4.4), and the other has $x = 0.047$ (PZT 4.7). The PZT compositions were first synthesized in the form of powders, with an average grain size on the order of micrometers, by "Chem-Prep" techniques [Voigt, 1998]. The powders were formed into slugs with Avicel, an organic cellulose-like filler material. The Avicel filler burned off during sintering of the slugs, leaving voids tens of micrometers in dimension. The sintered slugs have 93% of the theoretical density expected for the PZT compositions. For the stress experiments, the PZT slugs were machined into bars in the shape of right prisms, about one inch (2.5 cm) long and with an approximately square cross-section of about 0.4 inches (1.0 cm) on a side. The following table lists, by composition, the PZT bars on which stress experiments were carried out and provides their dimensions and the maximum stress applied during the experiment. Channel Industries performed the initial machining, and most of the bars were used in the dimensions (approximately 1.000 x 0.425 inch) as received from Channel Industries. However, two bars (PZT 4.4/SP12H-16 #14 and PZT 4.7/SP14B #15, see table), were further machined to reduce their cross-sections, so as to achieve a higher stress within the force limitations of the load frame. All bars were annealed at 600°C to reverse any FE-to-AFE transitions induced at the surface of the bars by stresses related to the machining.

Table 1 - Stressed PZT Bars

Bar Number	Dimensions, in.	Max Stress, MPa
PZT 98/2 (x=0.02) AFE Bars		
SP15A #11a	1.006 x 0.425 x 0.425	260
PZT 95.6/4.4 (x=0.044) FE Bars		
SP12H-16 #9	1.006 x 0.425 x 0.425	425
SP12H-16 #10	1.005 x 0.426 x 0.425	400
SP12H-16 #12a	1.006 x 0.426 x 0.425	400
SP12H-16 #14	1.005 x 0.400 x 0.399	500
PZT 95.3/4.7 (x=0.047) FE Bars		
SP14B #2	1.004 x 0.425 x 0.425	425
SP14B #7	1.004 x 0.425 x 0.425	425
SP14B #8	1.005 x 0.426 x 0.425	425
SP14B #15	1.004 x 0.399 x 0.399	500

Raman Measurements

Raman spectroscopy was performed using a triple spectrometer, which is comprised of two filter stages (to remove unshifted Rayleigh scatter at the laser frequency) and a spectrograph stage (to disperse the remaining light into its constituent frequencies). Using high groove density (1800 groove/mm) gratings, this instrument can record photons with frequencies very close (10 cm^{-1}) to that of the laser line and resolve frequencies within $3\text{-}4\text{ cm}^{-1}$ of each other. The 514 nm line from an argon ion laser provided the excitation light, which was focused through microscope optics to an approximately one micrometer spot on a PZT bar. Light backscattered off the PZT bars was collected by the microscope optics and transferred to the spectrometer, as is shown schematically in Figure 1. Light dispersed by the spectrometer spectrograph stage was imaged onto a charge-coupled device. The charge-coupled device is a type of imaging photon detector, which records the photon intensities at all the frequencies in the dispersed spectrum simultaneously. With 5 mW of laser intensity focused onto the bar, a spectrum could be recorded in 10 to 30 seconds.

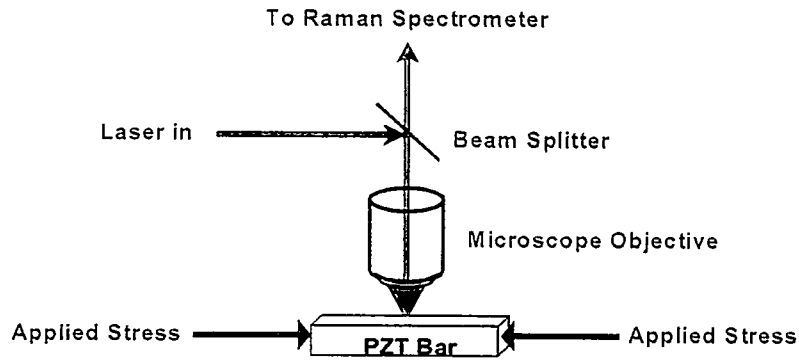


Figure 1. Schematic diagram of the stressed PZT/Raman spectroscopy experiment

A photograph of the apparatus, showing the major components (spectrometer, microscope and load frame holding the PZT bar) is shown in Figure 2. The load frame rests on the mechanical stage of the microscope. The PZT bar is hidden by cover plates on the load frame.

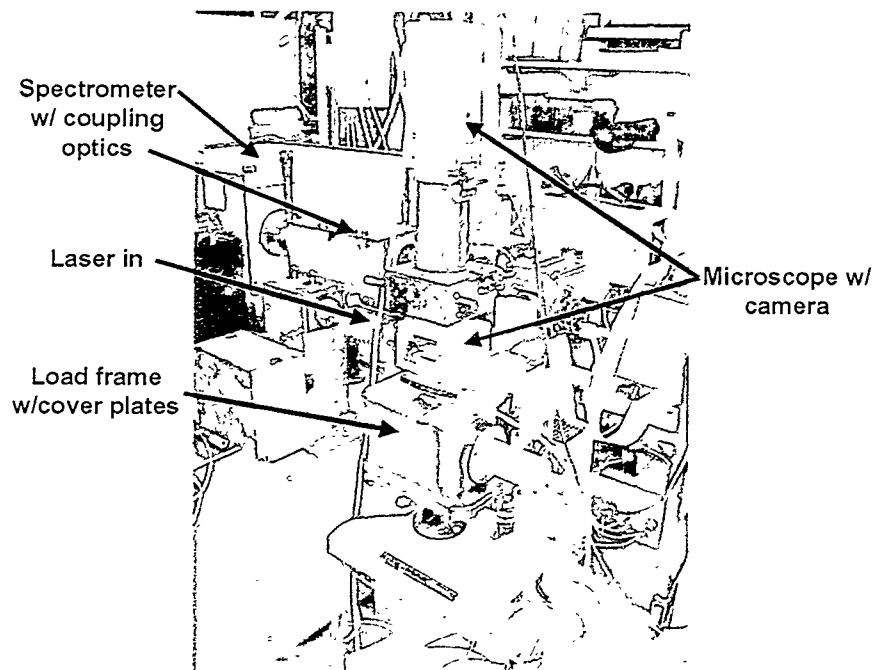


Figure 2. Photograph of the spectrometer, microscope and load frame.

The Load Frame

We designed and constructed a simple loading device having sufficient capacity to induce FE-to-AFE transformations in the PZT bars while being small enough to fit on the mechanical stage of the microscope used for micro-Raman analysis. This load frame is shown in Figure 3. The reaction frame was fabricated from an 8.9-cm long segment of rectangular steel tube. The tube has outside dimensions of 15.24-cm long by 10.16-cm wide, with a wall thickness of 0.95 cm. Load is applied to the test specimen with a 45 kN capacity, Enerpac hydraulic actuator (Model RC51), which is threaded into one end of the tube segment. At the other end of the steel tube, a shallow disc was machined out to centrally locate a 0-133.4 kN Sensotec load cell (Model TH A691-01). The load cell is held in place by a bolt that passes through the tube wall. Loading platens were fabricated for both the load cell and the actuator, to provide precise parallel alignment (uneven compressive loading of the brittle ceramic specimens could result in failure before onset of the transformation). The test specimens themselves were fitted with slightly oversized tungsten carbide endcaps in order to spread the load more evenly over the platens and prevent their indentation by the specimens. The loading apparatus is fitted with aluminum cover plates (not shown in Figure 3) which allow microscopic observation of the specimens but restrict the dispersal of ceramic fragments in the event of a catastrophic specimen failure. No such failures occurred during the experiments described in this report. The load frame apparatus and associated instrumentation are sufficiently portable that they could be easily transported to the Raman laboratory.

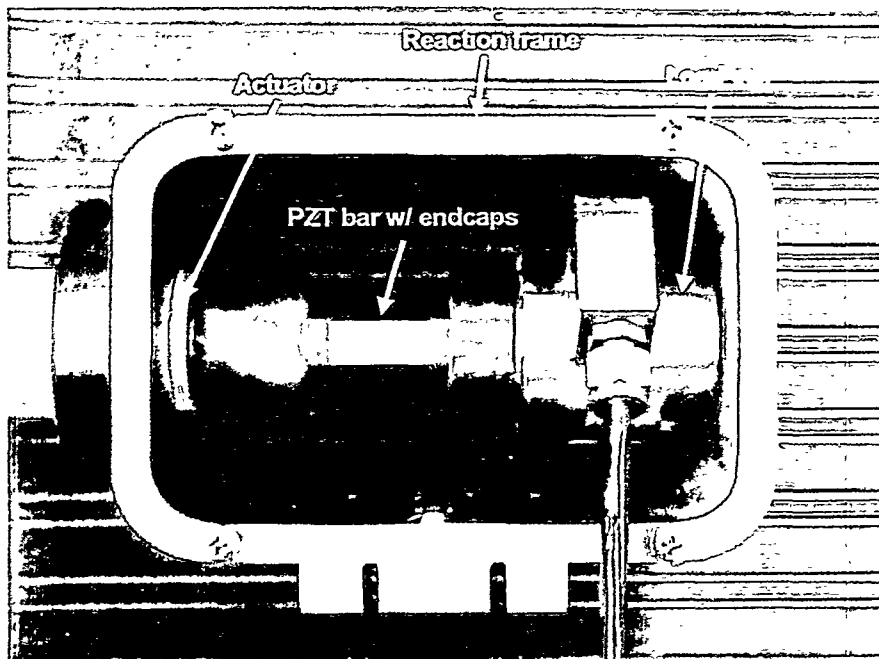


Figure 3. Load frame with PZT bar/endcaps mounted.

Coarse pressure was applied to the actuator using a hand-operated Enerpac hydraulic pump. Pressure was finely controlled using a hand-operated, small-bore intensifier. The fine control was used to set the pressure at which spectroscopic measurements were to be performed and to keep the pressure constant during those measurements. Some slight drop in pressure (and, hence, axial stress) did occur during the time intervals when spectroscopic analysis was being performed. This may have been caused by creep resulting from time-dependent dipole switching, FE-AFE transformation, leaks in the loading hydraulic system or some combination thereof. However, pressure could generally be held constant within a few megapascals (MPa) during the acquisition of Raman spectra.

In order to provide an independent measurement of the FE-to AFE transformation during uniaxial compression, axial and lateral strains were recorded using standard, foil-backed resistance strain gauges bonded to one rectangular face of each specimen. Use of more gauges would have been desirable so that effects of slightly eccentric loading could be averaged out. However, maintaining portability of our testing apparatus dictated keeping the number of gauges and associated instrumentation to a minimum. Both Fritz [1979] and Zeuch *et al.* [to be published] have shown that onset of the transformation is signaled when the normally-tensile, lateral strains actually begin to reverse owing to the 0.7-0.9% volumetric contraction that accompanies the polymorphic transformation. Volumetric strains can also be used as indicators for onset of the transformation during uniaxial compression. The axial strain measurements are necessary to compute the volume strain. The strain gauges were also used to identify any signs of premature failure. Cover plates on the load frame restricted wide dispersal of PZT fragments released by catastrophic failure, but a line-of-sight path to the microscope objective is necessary for the Raman measurements. Because of the possibility of damage to the microscope objective from PZT fragments released by catastrophic failure, the applied stress was not increased any further than the point at which stress/strain plots indicated potential catastrophic failure. In the absence of such indication, stress was applied up to the limit of the ability of the actuator to apply load. The experiment involving the (AFE) PZT 98/2 bar (SP15A #11a) was terminated at relatively low applied stress when anomalous strain and loading behavior were observed.

Signals from the strain gauges and load cell were digitized, converted to engineering units and stored on the hard drive of a portable Dolch, IBM-compatible PC using the data acquisition program DATAVG [Hardy, 1993]. Although lateral strains were measured in one direction, stress data were not corrected for changes in cross-sectional area. However, since lateral strains are typically less than 0.2% (true strains of 0.002), changes in cross-sectional area, and, hence, corrections for the true stress, amount to less than 1%. In this report, compressive strains are reckoned positive and tensile strains are negative, following the usual rock mechanics convention.

Raman Sampling of the PZT Bars

The optical microscope incorporated into the Raman spectrometer focuses the laser excitation beam onto a one micrometer spot on the surface of the PZT bar and collects light scattered from the illuminated area for analysis by the spectrometer. The microscope also has a video camera, which provides a real-time view of the sampled area and which allows us to accurately and reproducibly position the laser spot on a feature of interest. Figure 4 shows a frame captured from the video camera. The view in this frame shows the area of a PZT 4.7 bar (SP14B #8) from which Raman spectra were obtained as uniaxial stress was applied. This micrograph shows the porosity generally characteristic of the surfaces of the PZT bars. Note that individual PZT grains are not generally visible in the micrograph, but there is abundant topography from which to select and reproducibly locate features for Raman sampling. The arrows mark locations from which Raman spectra were obtained during the stress experiment. The laser beam was re-positioned to obtain a Raman spectrum at each location after each increment of applied stress. This procedure provided a set of spectra at all applied stresses for each location in one cycle of ambient-to-maximum-to-ambient stress for each bar. Different types of features were sampled. "Flat" locations are at the surface of the PZT bar, and they are sometimes associated with a "groove" or grooves from machining or polishing operations. We avoided flat locations on heavily grooved surface regions because of the possibility of residual stresses due to machining or polishing. "Shallow" locations are regions recessed from the surface (probably) 5 to 10 micrometers. "Deep" locations are recesses tens of micrometers from the surface. For all the PZT bars, all the locations sampled to obtain Raman spectra were within one, approximately 100 by 70 micrometer area, as illustrated for SP14B #8 in Figure 4.

Given the spatial resolution achieved by focusing the laser beam through a microscope objective (one micrometer horizontal, a few micrometers in depth) and PZT grains a few micrometers in dimensions, we expect that the Raman spectra reflect the structure of primarily one PZT grain. However, light scattering from grain boundaries and the possibility of inadvertently focusing the laser beam on a grain boundary are likely to add contributions from more than one grain to at least some of the Raman spectra.

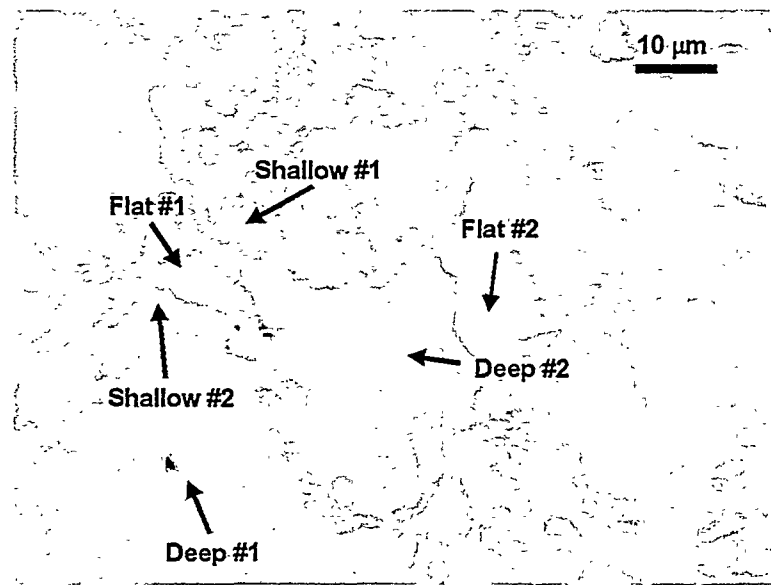


Figure 4. Micrograph of area of PZT 4.7 (SP14B #8) sampled by Raman during stress experiment

Stress-Strain Data

Figures 5 to 13 show the stress-strain data for the nine experiments. The strains are plotted as the axial (along the direction of applied stress), lateral (perpendicular to the direction of applied stress) and volume components (ε_a , ε_l , and ε_v , respectively). The volume strain is calculated from the measured axial and lateral strains. Positive strains are compressive, and negative strains are tensile (expansion or dilatation). The axial dimension typically becomes smaller, while the lateral dimension expands, with axial applied stress.

The stress experiment involving the AFE-phase, PZT 98/2 bar (SP-15A #11A, Figure 5) was terminated at relatively low applied stress because excessively large lateral strains (and audible cracking noises) signaled that failure was imminent. The volumetric strain data show the classic reversal from compression to dilatation that indicates the growth of cracks. Other than the anomalous lateral strain excursions, there is no evidence in the stress-strain data for a phase transformation, such as occur when FE phase compositions are stressed.

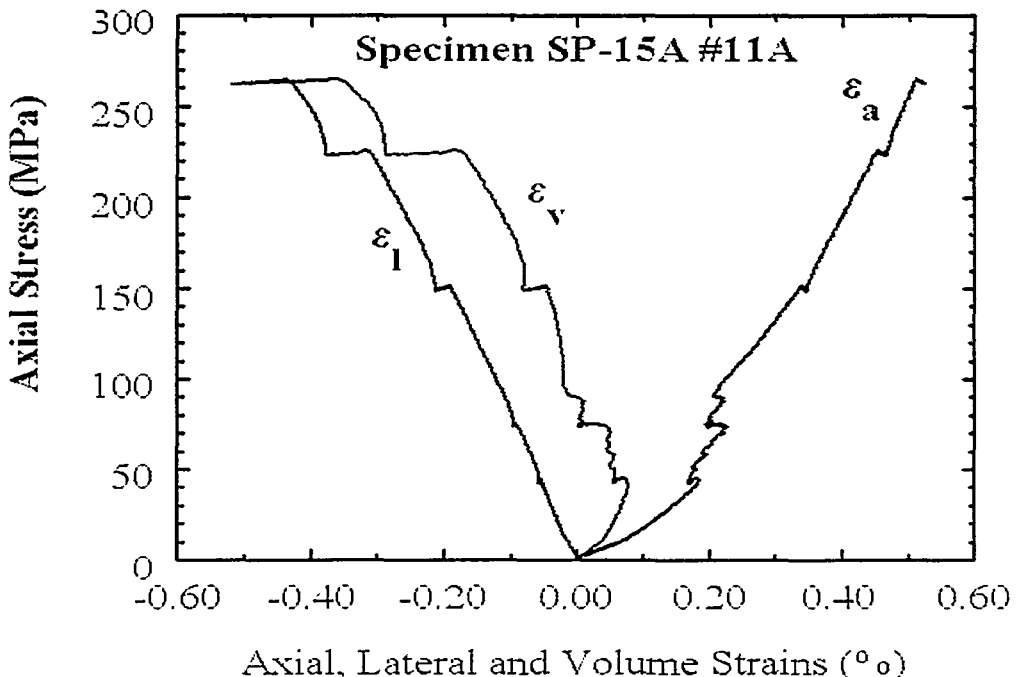


Figure 5. Stress-strain data for SP-15A #11A, a bar of PZT 98/2

The stress-strain data from two of the stress/Raman experiments involving FE-phase compositions showed notable anomalies. The axial strain gauge for PZT 4.4 bar SP12H-16 #14 (Figure 9) exhibited transient noise at applied stresses of 350 – 400 MPa but recovered at higher stresses. The overall shapes of the stress-strain curves from this experiment are consistent with those from the other stress/Raman experiments on FE-phase PZT bars. In the experiment involving the PZT 4.7 bar SP14B #8 (Figure 12), excessive noise was encountered from the axial strain gauge. This partially subsided late in the experiment, so we plot those data along with the calculated volume strain. The lateral strain data does not show the anomaly.

The stress-strain curve shapes from the experiments involving FE-phase PZT bars (Figures 6-13) display general features which are consistent with those of Fritz (1979) and Zeuch *et al.* (1999; in press). Some of the experiment-to-experiment variability in the plots may be due to the relative simplicity of our load frame, the slow (and highly variable) rate at which specimens were loaded and the limited amount of strain gauge instrumentation on the PZT bars. Axial and lateral strains are roughly linear up to stresses of 75-100 MPa. Minor nonlinearities in this stress range may be due to eccentric loading and premature triggering of the FE-AFE transformation at localized stress concentrations. At 75-100 MPa compressive axial and tensile lateral strains become markedly nonlinear and anomalously large. The volume strain remains approximately linear. Dipole switching, rather than onset of the FE-AFE transformation, is believed to be the cause of these low-stress nonlinearities. At approximately 150 MPa the rate of increase in the compressive volume strain accelerates, departing

appreciably from linearity, and there is a slower rate of increase in the tensile lateral strain, presaging an eventual reversal towards compression. Accelerated volume compression and the reversal of lateral expansion are indicators of the FE-to-AFE transformation, since the AFE phase has a smaller unit cell. The stress-strain data suggests that the FE-AFE transformation begins at 150 MPa applied stress and continues throughout the stress range of this experiment (Zeuch *et al.*, 1999; *in press*). The apparent transformation stress for these unpoled, "chem-prep" ceramic specimens (about 150 MPa) appears to be somewhat lower than that for the unpoled "mixed-oxide" ceramic (200-250 MPa) examined by Zeuch *et al* (1999; *in press*).

The saw-toothed offsets in the axial and volumetric strain records of the experiments using the FE-phase PZT bars correspond to times when the stress was maintained approximately constant while spectroscopic measurements were performed. To a lesser extent, these offsets are also present in the lateral strain data. The continued volume contraction at constant stress indicates that a time-dependent transformation was occurring. The stress-strain plot for the PZT 4.4 bar (SP12H-16) # 12A (Figure 6) does not show the saw-toothed offsets because, in this experiment, the stress was cycled from its minimum to maximum to minimum values without intermediate steps.

Differences between the stress-strain plots for different PZT bars suggest varying responses to applied stress. Lateral strain reversals are well-developed in the stress-strain plots for the PZT 4.4 bars (Figures 6 - 9) and the PZT 4.7 bar (SP14B) # 15 (Figure 13) which was stressed to 500 MPa. They are less-developed in the stress-strain plots for the for PZT 4.7 bars (SP14B) # 2, 7 and 8 (Figures 10 – 12). The stress-strain plots for PZT 4.4 bars (SP12H-16) # 10 and 14 (Figures 7 and 9) show little evidence for dipole switching compared to the plots for the other bars, and the volume strain data for PZT 4.7 bar (SP14B) #7 (Figure 11) suggests a relatively high FE-to-AFE transformation stress. Some of this variability may be due to the limitations on the strain gauge instrumentation, but, as we shall discuss, the variations in the stress-strain data are consistent with those seen in the stress-Raman data.

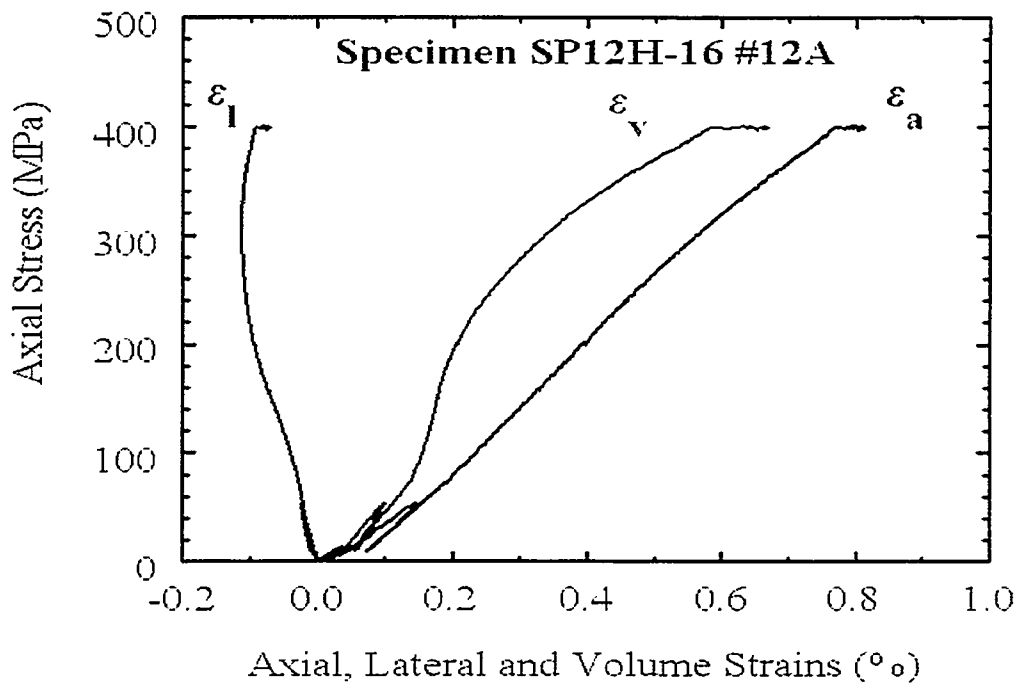


Figure 6. Stress-Strain data for SP12H-16 #12A, a bar of PZT 4.4

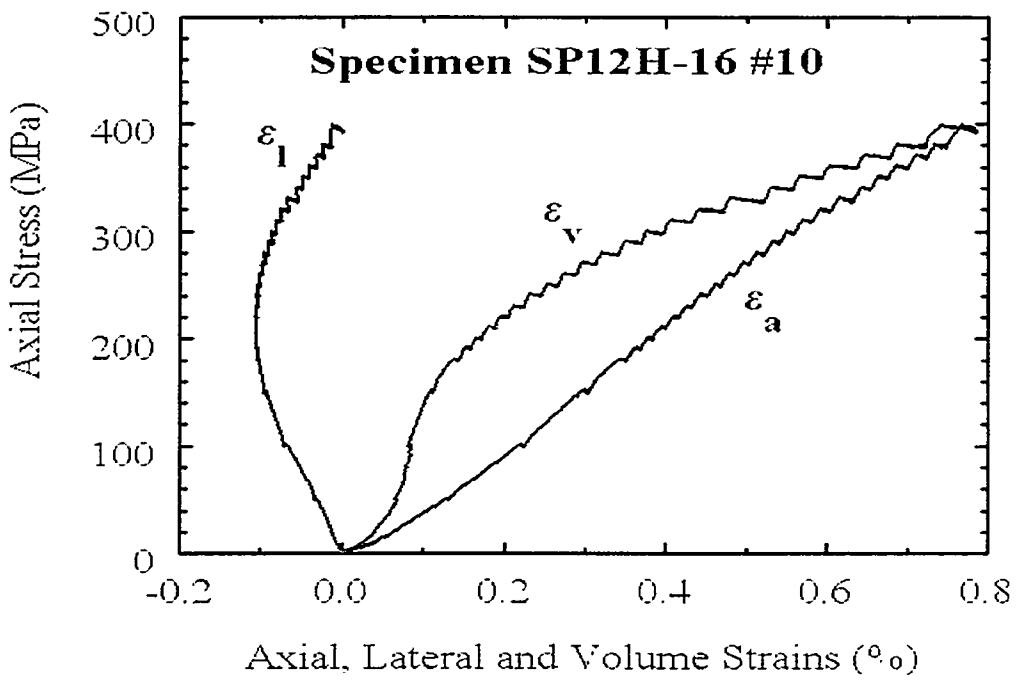


Figure 7. Stress-strain data for SP12H-16 #10, a bar of PZT 4.4

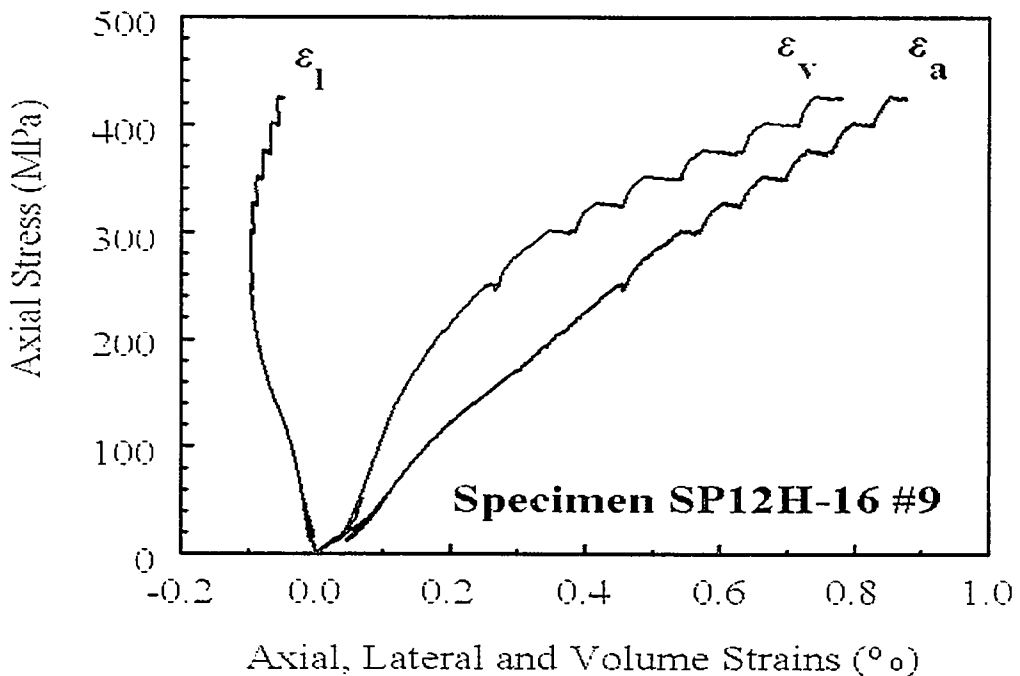


Figure 8. Stress-strain data for SP12H-16 #9, a bar of PZT 4.4

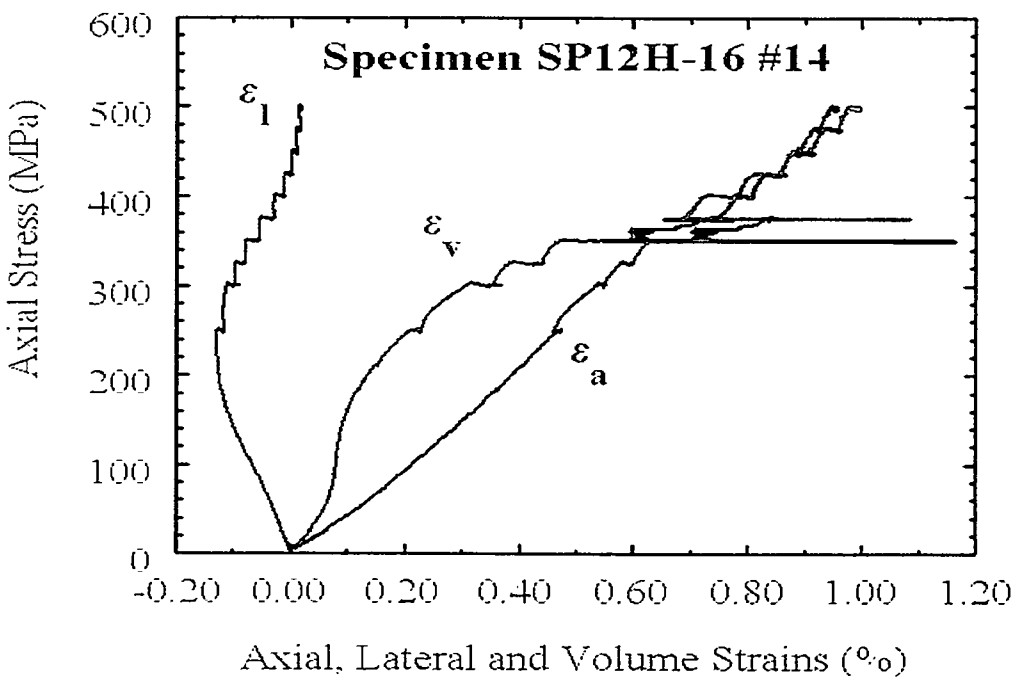


Figure 9. Stress-strain data for SP12H-16 #14, a bar of PZT 4.4

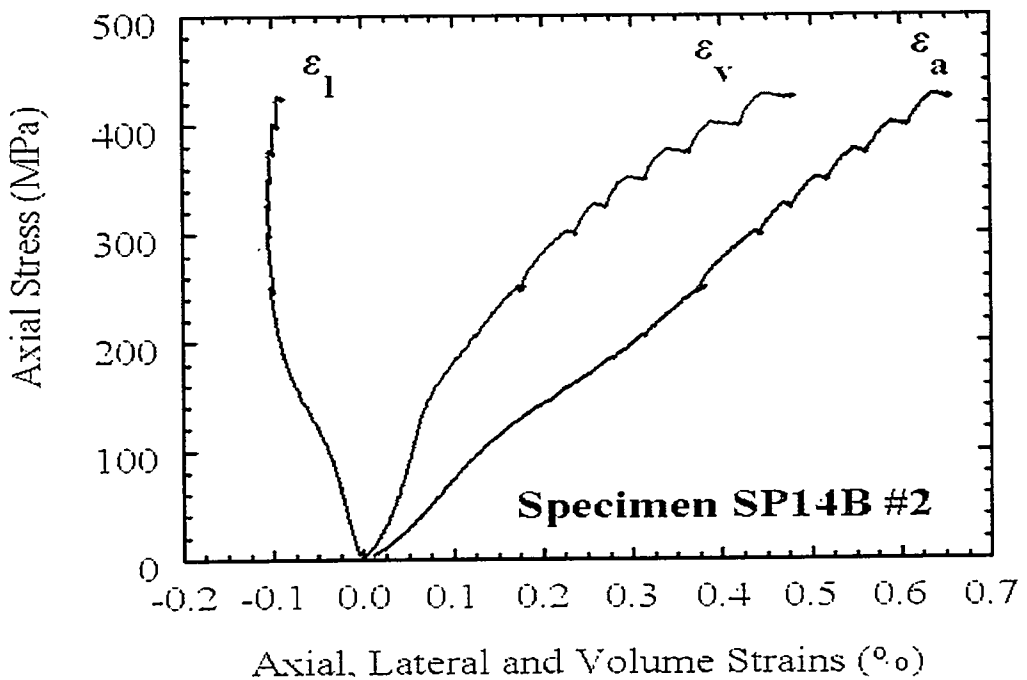


Figure 10. Stress-strain data for SP14B #2, a bar of PZT 4.7

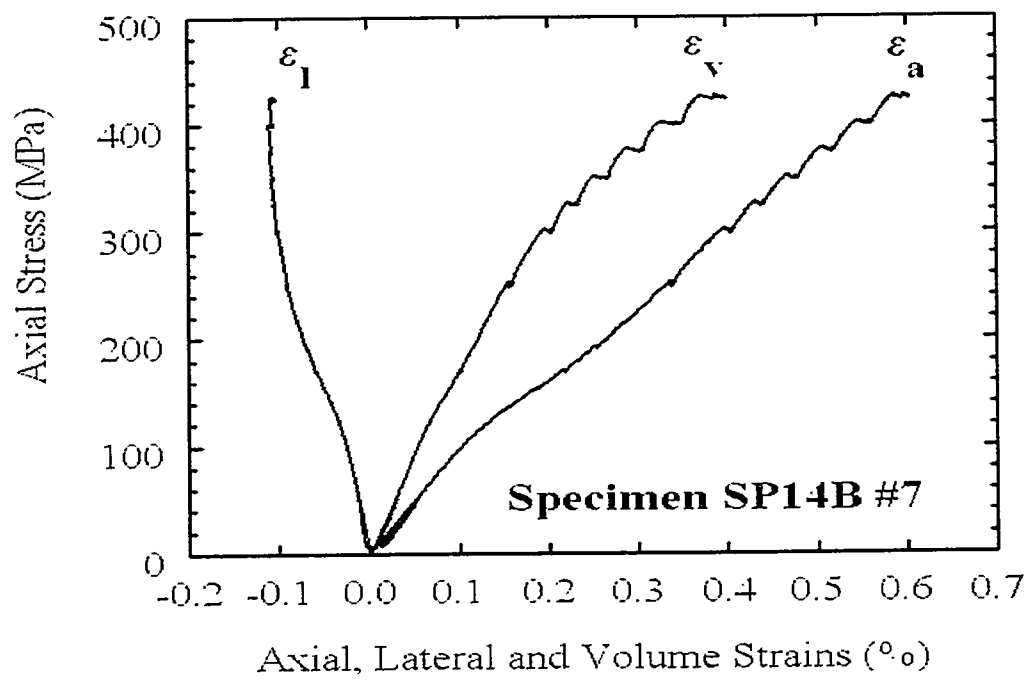


Figure 11. Stress-strain data for SP14B #7, a bar of PZT 4.7

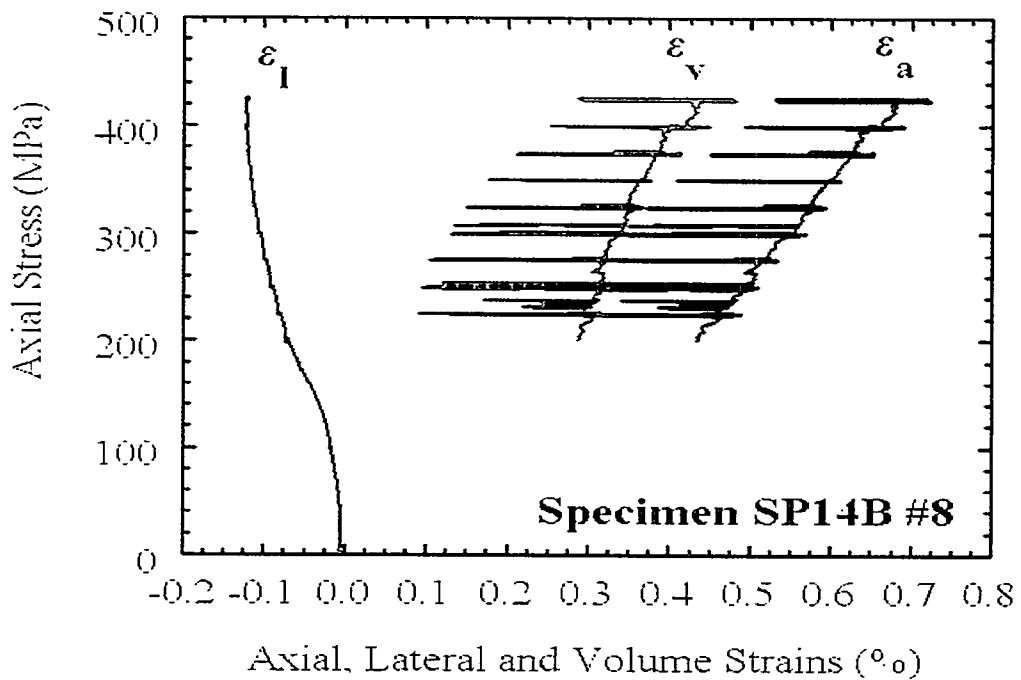


Figure 12. Stress-strain data for SP14B #8, a bar of PZT 4.7

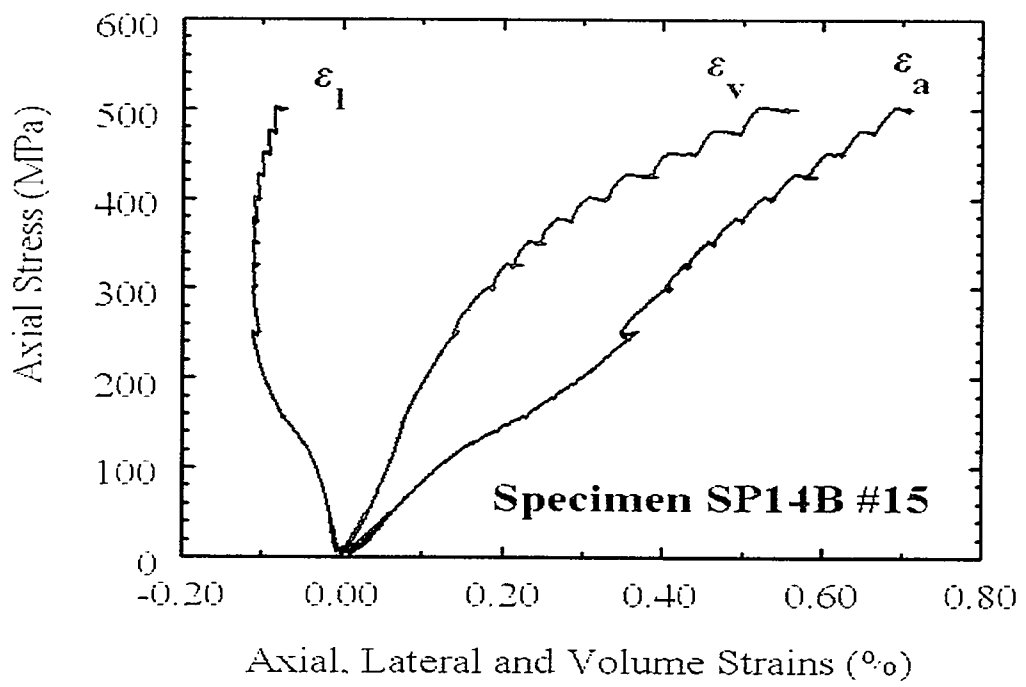


Figure 13. Stress-strain data for SP14B #15, a bar of PZT 4.7

Raman Spectra from AFE and FE Phases of PZT

The Raman effect is an inelastic scattering technique, in which a photon in the beam of monochromatic (single frequency) photons from the laser source interacts with an electron cloud in a bond linking atoms in the material being illuminated. Most of the incident photons rebound elastically (with the same frequency as the incoming photons) as Rayleigh scatter. About one in a million photons scatter inelastically by interacting with the phonons (quanta of vibrational energy) intrinsic to the crystal structure of the material being illuminated. If the photon loses energy due to this interaction, it is said to be (Stokes) Raman-shifted. This energy loss (or "Raman shift") is measured in frequency units (cm^{-1}) and is the same as the frequency of the atomic vibration with which it interacted. If, as is customary, we plot the intensity of the inelastically scattered photons versus frequency, with the initial laser frequency as 0 cm^{-1} , then the frequency axis is in Raman shift units, and peaks in the spectrum correspond directly to vibrational modes of the atoms in the material being illuminated. Raman spectra look generically similar to infrared absorption spectra, but the same vibrational bands are not necessarily present in both types of spectra.

We obtained Raman spectra of PZT compositions with known phases as references for comparison with spectra of PZT bars under stress. In Figure 14 we show the low frequency portions of the Raman spectra from well-characterized (by x-ray diffraction) bars of nearly pure AFE and FE phases. The AFE spectrum is from a PZT 98/2 ("PNZT 4/27/99"), and the FE spectra are from a PZT 4.4 ("SP12H lot 9819 #10") and a PZT 4.7 ("SP14B lot 9828 #16"). The low frequency regions of the PZT spectra provide the most discrimination between the AFE and FE phases. The vibrational modes in this region are probably due to motions of the heavy metal cations in PZT. Particularly in the band structure near 50 cm^{-1} , the spectrum of the AFE material in Figure 14 shows significant differences from the spectra of the two FE materials. Any differences between the spectra of the two FE materials are relatively subtle. We based our analysis of phase changes in PZT materials under uniaxial stress on a comparison with reference spectra, including those shown in Figure 14.

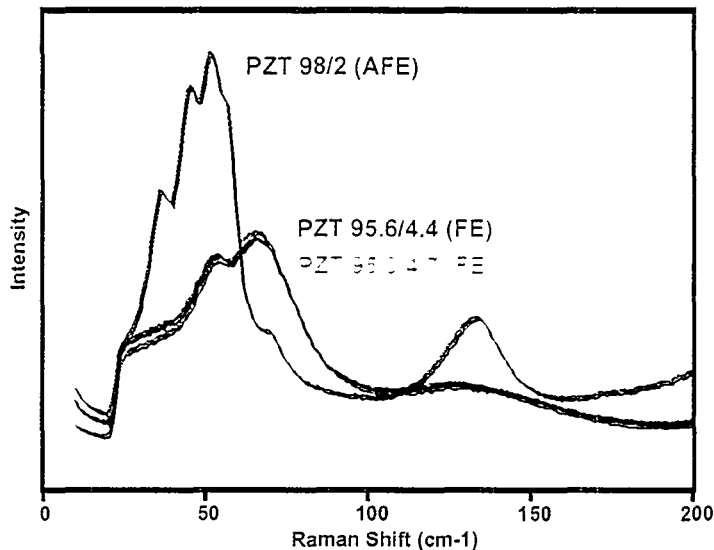


Figure 14. Raman spectra of the AFE and FE phases of reference PZT compositions.

Extraction of FE/AFE Phase Information from the Raman Spectra

The problem facing us in processing and interpreting the Raman spectra from the stress experiments is how to extract information on FE-to-AFE phase changes as a function of applied stress from the approximately 500 spectra collected during stress/Raman experiments on nine PZT bars. Our solution is to define an "FE coordinate", which is a measure of the relative amount of FE phase in the area of the PZT bar sampled by the laser excitation beam. We define the FE coordinate to be 1.00 for a (nearly) pure FE phase and to be 0.00 for a pure AFE phase. Six Raman spectra, two each from well characterized PZT 98/2, PZT 4.4 and PZT 4.7 bars, were selected to form a calibration set against which spectra from stressed PZT bars are compared. Three of the spectra used in the calibration set are shown in Figure 14.

The calibration calculations and the prediction of FE coordinates from the Raman spectra used multivariate statistical techniques employing partial least squares regression [Galactic, 1999]. These data analysis techniques compare whole spectra or selected portions thereof. In processing a set of spectra, say, the calibration set of PZT Raman spectra, a set of spectra-like factors is calculated. Appropriately scaled and summed, these factors reproduce any spectrum in the set. When regressed against some property associated with the spectra (in our case the FE coordinate), the factors and the values used to scale them form something analogous to a calibration curve, which can be used to predict the property (the FE coordinate) in "unknown" spectra. In this way FE coordinates were calculated for the spectra obtained in the stress/Raman experiments.

From our experience with Raman spectroscopy, we know that the shapes and relative intensities of Raman bands in a spectrum are highly reproducible. However, the overall intensity of the Raman spectrum varies with the size and shape of the volume illuminated. Because of light scattering at grain boundaries, this effect is especially important for grains of micrometer dimensions. For this reason, the integrated intensities of all of the Raman spectra were normalized prior to statistical analysis. This normalization imposes the assumption that the Raman scattering efficiencies of the FE and AFE phases are the same. It is probably not the case that they are the same, but, given the inability to obtain single FE and AFE crystals large enough to minimize the effect of internal light scattering, we have not been able to determine their actual Raman efficiencies. Strictly speaking, the FE coordinates are not quantitative measures of the fraction of FE phase in the volume of PZT sampled. They are believed to be semi-quantitative measures of the FE fraction and good indicators of the relative magnitude of FE-AFE transitions.

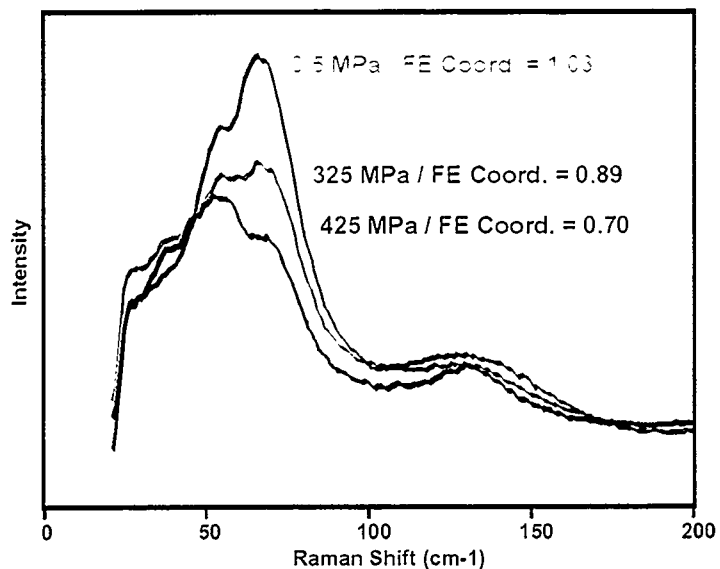


Figure 15. Raman spectra from location Deep #1 (PZT 4.7, SP14B #8) at applied stresses of 3.5, 325 and 425 MPa.

Figure 15 shows three Raman spectra, obtained at applied stresses of 3.5, 325 and 425 MPa, from the Deep #1 location of PZT 4.7, SP14B #8 (see Figure 4). With increasing applied stress, the spectra clearly show a transition from an FE-like spectrum to one with contributions from bands (e.g., near 50 and 140 cm⁻¹) in the AFE reference spectrum (see Figure 14). FE coordinates, calculated for each spectrum using the multivariate partial least squares analysis described previously, are also shown in Figure 15. As expected, the FE coordinate decreases as the AFE contribution to a spectrum increases.

Data from the PZT 98/2 Stress/Raman Experiment

Uniaxial stress up to 260 MPa was applied to a bar of AFE-phase PZT 98/2 (SP15A #11a). The maximum stress was limited to 260 MPa because the stress/strain plot indicated that the bar was near catastrophic failure at this stress. This experiment was primarily a baseline test of the experimental procedure. No phase changes in the AFE PZT 98/2 were expected at the stresses achievable with the load frame.

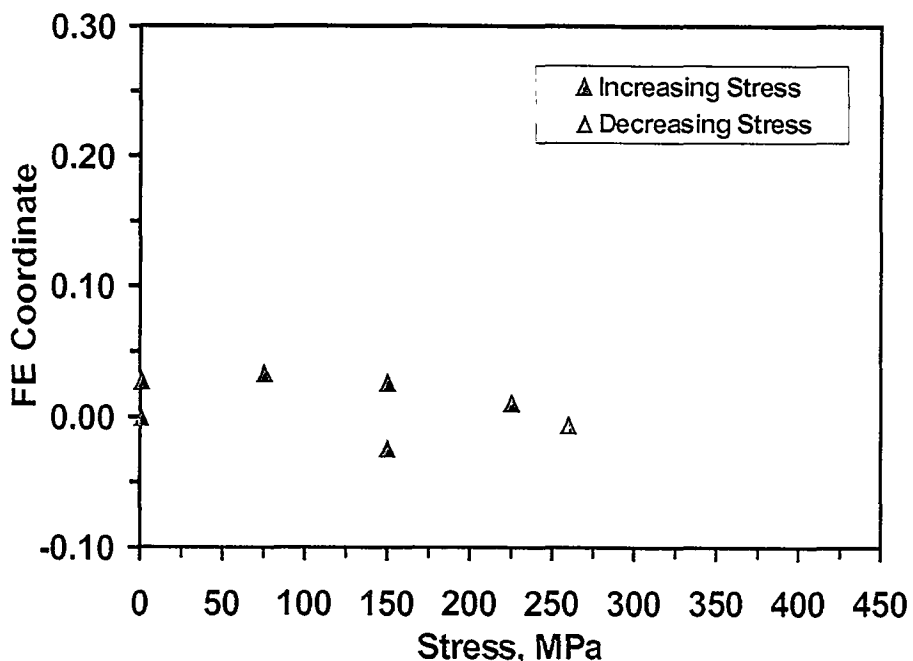


Figure 16. FE coordinates versus applied stress for a bar of AFE-phase PZT 98/2 (SP15A #11a)

Figure 16 shows the results of the stress/Raman experiment on the PZT 98/2 bar. Only one location was monitored. As expected, the FE coordinate is near zero throughout the experiment, although it may be experiencing a small decrease with increasing stress, indicating a slight increase in AFE structural characteristics. Also, there may be a slight hysteresis in the FE coordinate as the stress is reduced to near ambient conditions. This experiment provided a complete test of our experimental procedures and helped to confirm the validity of our data extraction

Data from the PZT 4.4 Stress/Raman Experiments

Figures 17 through 20 plot FE coordinates versus applied stress for four stress/Raman experiments involving bars of PZT 4.4 from the SP12H-16 set (see Table

1). The results of the experiment involving bar #12A are shown in Figure 17. In this experiment ten locations were selected and their Raman spectra obtained at a nominal stress of a few MPa and at 400 MPa, which is near the limit of the achievable stress for a bar with the cross section of #12a (Table 1). FE coordinates were calculated from the Raman spectra, as noted in an earlier section.

At all of the locations sampled on the PZT 4.4 bar (SP12H-16) #12A, there was some reduction in FE coordinate at the maximum stress, but, at some locations, e.g., Flat #1 and Deep #2, the change is relatively large (>0.1 unit), while at others, e.g. Flat #3 and Shallow #1, the change is relatively small (0.02 to 0.04 unit). The average change in FE coordinate with 400 MPa of applied stress is -0.072 ± 0.033 units. This dispersion in the FE coordinate change for the same macroscopically applied stress suggests that either the stress field at the micrometer scale is not homogeneous or that the response of PZT grains to a local stress is not uniform, say, due to grain orientation with respect to the stress tensor; or it is possible that both of these factors are involved. We will show that this nonuniform response to applied stress is a general characteristic of the PZT bars.

The average change of FE coordinate of -0.072 units indicates that there is only partial conversion from FE to AFE phase at these stress conditions. Again, there may be more than one factor that limits the implied phase change: an applied stress of 400 MPa may not be sufficient to produce a total FE-to-AFE transformation; or the Raman spectrum of the AFE phase in PZT 4.4 may not be as distinctively different from its FE phase as is the Raman spectrum of (AFE) PZT 98/2.

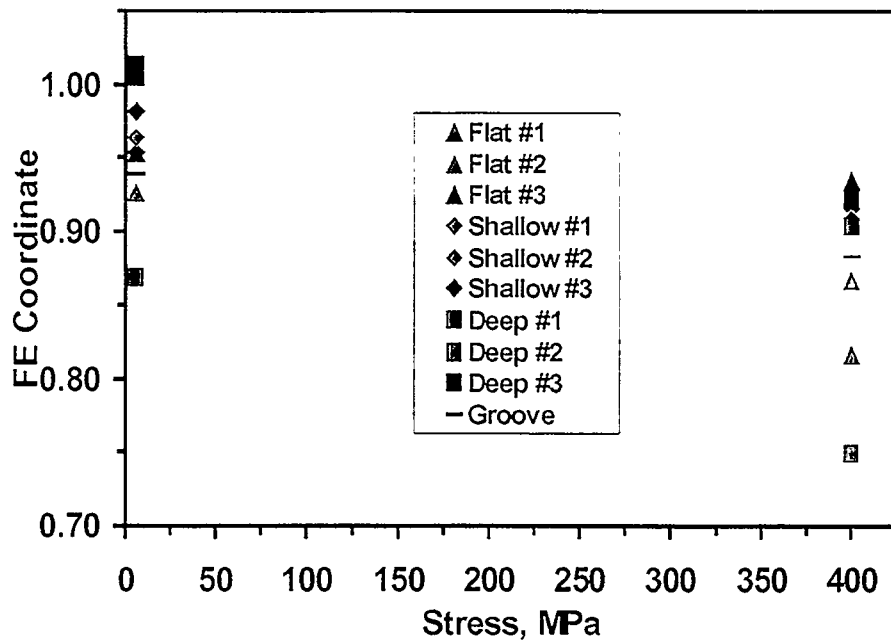


Figure 17. FE coordinates versus applied stress for a bar of FE-phase PZT 4.4 (SP12H-16 #12a)

In carrying out the stress/Raman experiment on PZT 4.4 bar (SP12H-16) #10, we took a different approach, obtaining Raman spectra at three locations while applying stress in relatively small increments. The FE coordinate versus stress plot is shown in Figure 18. Several points are noteworthy concerning this data. First, note that, for all three locations, the general decrease in FE coordinate (implying an FE-to- AFE transition) begins at 200 to 300 MPa of applied stress. As with bar #12A (Figure 17) the magnitude of FE coordinate change is significantly different at for different locations. Also, as the applied stress increases, the value of the FE coordinate does not follow a smooth curve but shows erratic variation with increments in stress. This variability is especially high for the Shallow location. In obtaining FE coordinates from the Raman spectra, the spectra are first normalized, and the FE coordinate calculation depends only on the highly reproducible frequencies, shapes and relative intensities of the Raman bands. Therefore, we do not believe that measurement error is the cause of this variability. Rather, the variability is probably due to grain boundary effects or the slipping of grains against each other. If we happen to focus the laser beam on or very near a grain boundary, small inaccuracies in reproducing the position of the focus spot from stress increment to stress increment can magnify scattering effects and result in sampling of an adjacent grain, which may not have the same FE/AFE ratio as its neighbor. Slippage of grains against each other may temporarily relieve stress on one

of the grains, resulting in a reversal of the FE-to-AFE transition. Both effects may be in operation, and the presence of either one suggests that, at the microscopic level, the FE-to-AFE transition can be chaotic rather than uniformly progressive. Note that grains sliding against each other, while relieving stress on one grain (increases FE coordinate), can increase the stress on another (decreases FE coordinate). Both types of single point excursions are present in the data shown in the FE coordinate plots.

At intermediate (50 – 250 MPa) applied stresses the FE coordinates (again, Figure 18) increase, implying that the phase has more FE character. This behavior has been noted for at least some locations in most of the PZT bars which were subjected to stress/Raman experiments. We do not believe that this increase in the FE coordinate is an experimental artifact, but we do not have an explanation of why it should occur.

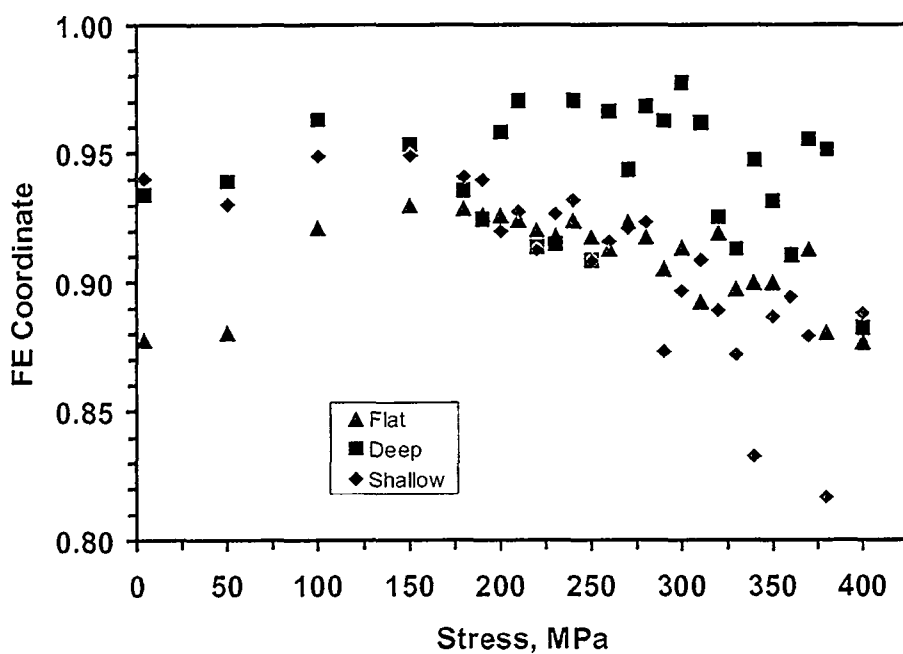


Figure 18. FE coordinates versus applied stress for a bar of FE-phase PZT 4.4 (SP12H-16 #10)

Plots of FE coordinates versus applied stress for PZT 4.4 bars (SP12H-16) #9 and #14 are shown in Figures 19 and 20, respectively. A maximum stress of 500 MPa was achieved for bar #14 because its cross section had been reduced (see Table 1). In these figures the results from different types of locations (Deep versus Shallow) are plotted separately to make it easier to follow the variation of the FE coordinate of individual locations. Our data does not indicate that Flat, Deep or Shallow locations respond, on average, significantly differently to the applied stress.

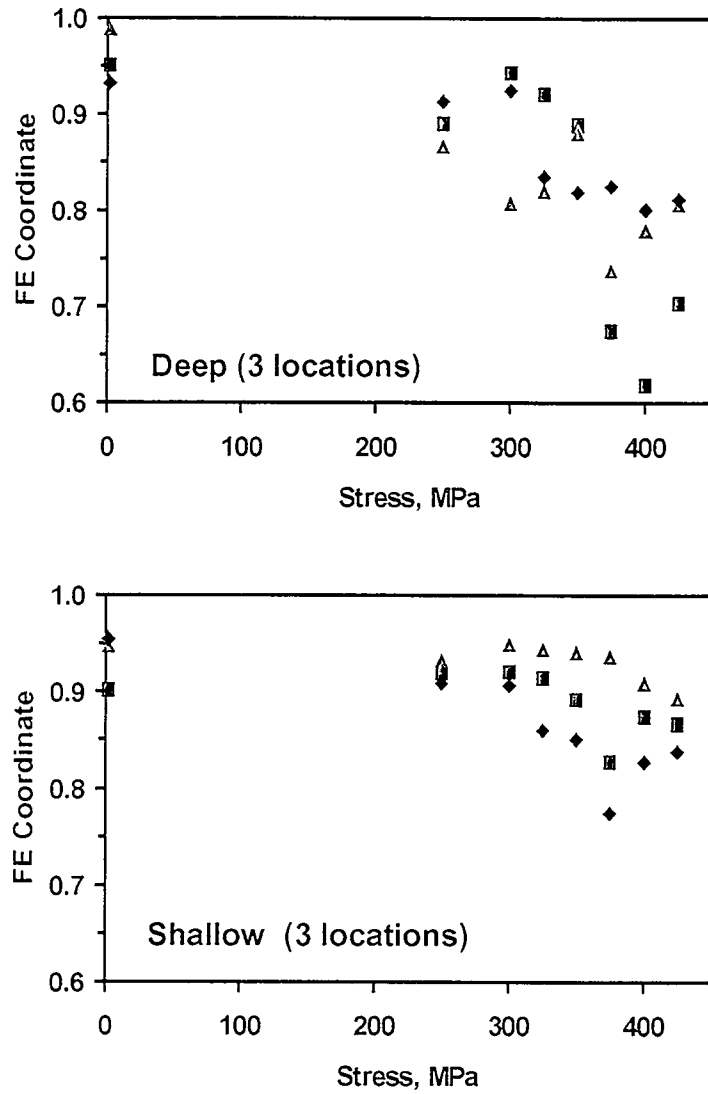


Figure 19. FE coordinates versus applied stress for a bar of FE-phase PZT 4.4 (SP12H-16 #9) with deep and shallow locations plotted separately

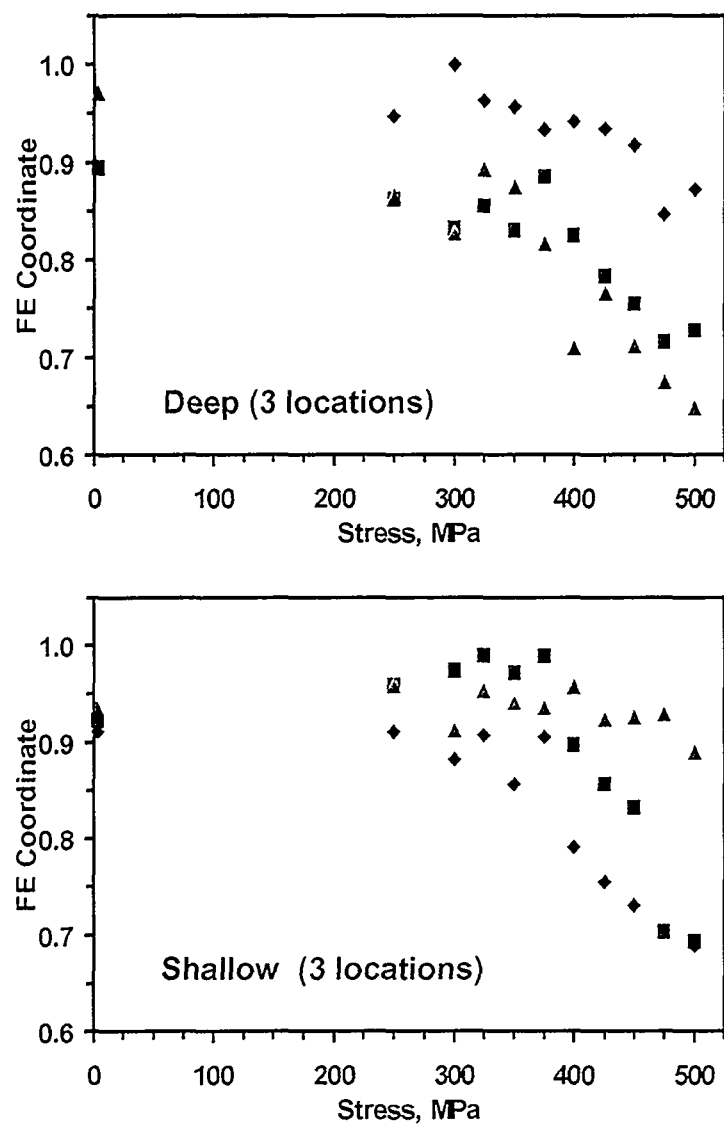


Figure 20. FE coordinates versus applied stress for a bar of FE-phase PZT 4.4 (SP12H-16 #14) with deep and shallow locations plotted separately

The FE coordinates for PZT 4.4 bars (SP12H-16) # 9 and #14 (Figures 19 and 20) show the same general response to uniaxial stress as the FE coordinates for PZT 4.4 bars (SP12H-16) # 12A and # 10 (Figures 17 and 18).

1. a slight majority of the locations show significant (>0.1 unit) decreases in their FE coordinate (compared to the initial value), the downward trend beginning between 200 and 300 MPa of applied stress;
2. a minority of locations have a similar FE coordinate at the highest applied stress as at the lowest, but even these are trending down at the highest applied stress, after an increase in their FE coordinate at intermediate applied stress;
3. the FE coordinate values vary significantly from location to location;
4. the progression of FE coordinate values with increasing stress sometimes shows single point excursions, which are probably related to variations in localized stress from slippage of grains against each other;
5. and the downward trend in FE coordinate continues when the stress increases past 400 MPa to 500 MPa (Figure 20).

Another interesting aspect of the FE coordinate data is its behavior after the applied stress is relieved. Raman spectra were routinely obtained, after release (to a few MPa) of the maximum applied stress, at the same locations monitored during the course of the stress/Raman experiment. At most locations the FE coordinate was within 0.05 unit of its initial (low stress) value. For some of the locations which had exhibited a significant decrease in FE coordinate by the maximum stress, the FE coordinate did not recover to its initial value. For example, four (of the six total) locations monitored on bar #14 (Figure 20) showed a large (>0.1) decrease in FE coordinate with applied stress. The FE coordinate from three of these four locations recovered to within 0.05 unit of the initial value when the stress was released. At one location (the Deep location plotted with triangles in Figure 20) the initial Fe coordinate was 0.97, and it decreased to 0.65 at 500 MPa of applied stress. After release of the stress, the FE coordinate increased only to 0.82, still 0.15 unit below the initial value. It is not known whether these "non-recovering" sites have undergone transitions to stable or quasi-stable AFE phases or whether a localized stress remains when the macroscopically applied stress is released.

Data from the PZT 4.7 Stress/Raman Experiments

Fe coordinates versus applied stress for bars of FE phase PZT 4.7 are shown in Figures 21 through 24. This data is the result of stress/Raman experiments performed on bars #2, #7, #8 and #15 from series SP14B (see Table #1). Bar #15 was reduced in cross section compared to the other bars and achieved a higher maximum stress (500 versus 425 MPa).

The Fe coordinate versus stress plots for the PZT 4.7 bars are generally comparable to those from the PZT 4.4 bars, with some notable exceptions. First, only

three of seventeen locations monitored on the bars to which a maximum stress of 425 MPa was applied (Figures 21 – 23) showed a significant (>0.1 unit) decrease in FE coordinate at the maximum stress. None of the locations monitored on PZT 4.7 bar (SP14B) #2 (Figure 21) showed a significant decrease in FE coordinate. Of the locations monitored on PZT 4.7 bar (SP14B) #8 (Figure 23), four showed not only no overall decrease in FE coordinate but also had relatively little point-to-point variation in the FE coordinate. One location on PZT 4.7 bar (SP14B) #8 (the Deep location plotted with a rectangle) showed minimal change in its FE coordinate until it abruptly began to decrease at 325 MPa. For the PZT 4.4 bars, a majority of the locations monitored exhibited a significant decrease in FE coordinate.

The FE coordinate versus stress data from PZT 4.7 bar (SP14B) #15 (Figure 24), which was stressed to 500 MPa, suggests why less change in FE coordinate is seen with the PZT 4.7 bars compared to the PZT 4.4 bars. All of the locations monitored on bar #15 show a distinct downward trend in FE coordinate, but it is apparent only in the region of 400 – 500 MPa stress, while most of the PZT 4.7 bars of the SP14B series experienced a maximum stress of 425 MPa. It appears that the onset of the FE-to-AFE transition occurs in the region of 300 – 350 MPa stress for the PZT 4.7 bars, as compared to 200 – 300 MPa for the PZT 4.4 bars. This change in the dependence of the FE-to-AFE transition on the stress is not unexpected, since the PZT 4.7 composition is further from the FE/AFE phase boundary than the PZT 4.4 transition and should be more stable with respect to stress.

Another difference between the PZT 4.7 and PZT 4.4 FE coordinate versus stress data is in its point-to-point variability. As typified by the plots from PZT 4.7 bar (SP14B) #8 (Figure 23), the data from the PZT 4.7 bars shows relatively few of the “excursions” in FE coordinate values more commonly occurring in the data from the PZT 4.4 bars (Figures 17 – 20). We attributed these excursions, at least partially, to slippage of PZT grains against each other, with attendant changes in local stress. While such slippage is expected to occur also in the PZT 4.7 bars, their composition should make the FE phase more stable with respect to changes in stress.

The FE coordinate versus stress data from the PZT 4.7 bars paints the same general picture as the PZT 4.4 bars. Rather than a progressive, homogeneous transition from the FE to the AFE phase as uniaxial stress increases, individual grains are present with different initial FE/AFE characteristics and transform to the FE phase at different macroscopically applied stresses; or, they may not transform at all. Local variations in stress at the microscopic scale, differences in grain structure and FE phase domain orientation, plus slippage of grains against each other, probably all contribute to this seemingly chaotic situation.

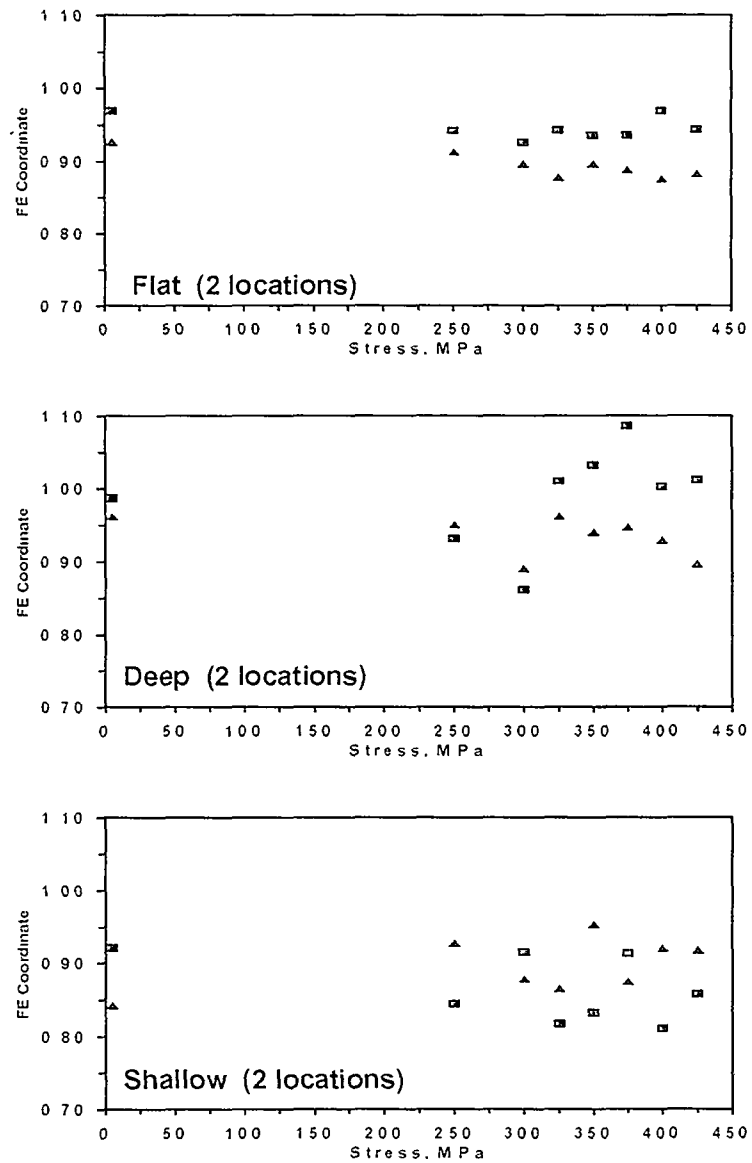


Figure 21. FE coordinates versus applied stress for a bar of FE-phase PZT 4.7 (SP14B #2) with flat, deep and shallow locations plotted separately

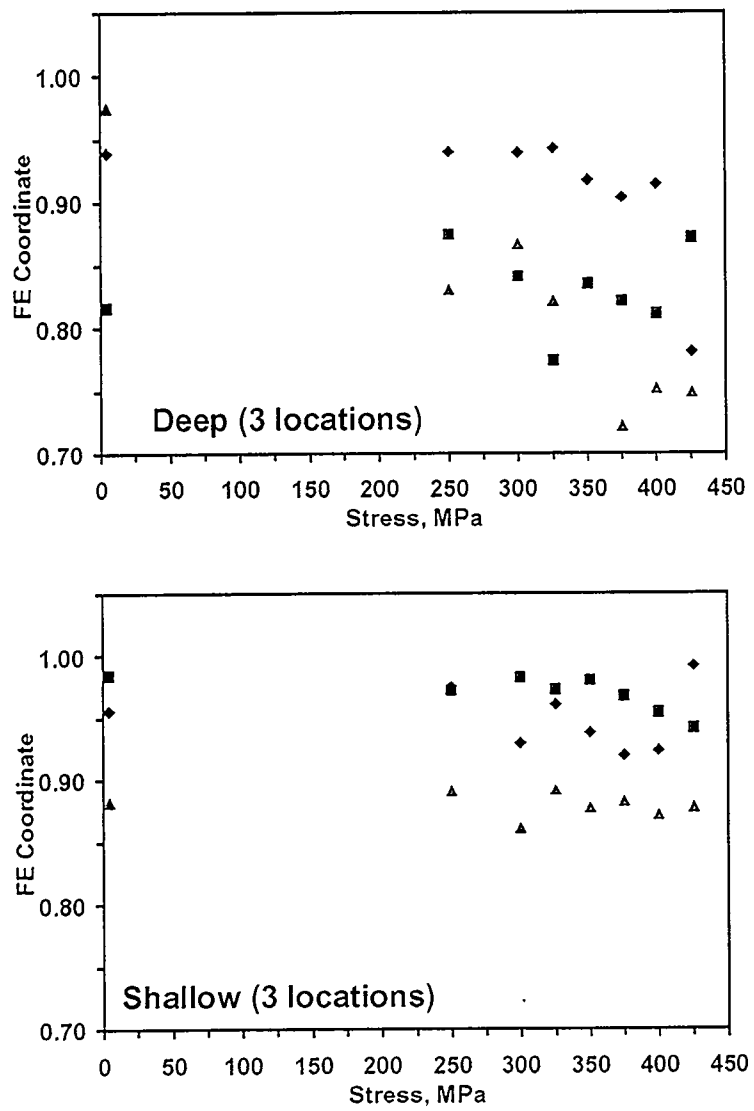


Figure 22. FE coordinates versus applied stress for a bar of FE-phase PZT 4.7 (SP14B #7) with deep and shallow locations plotted separately

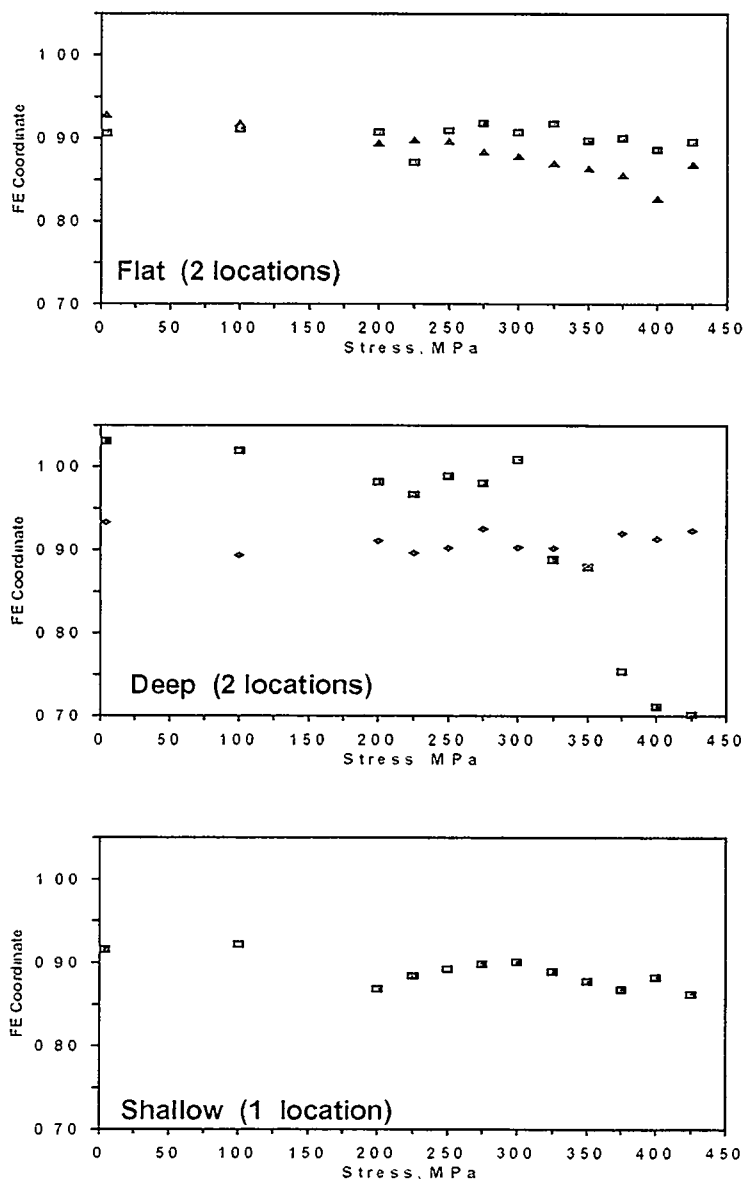


Figure 23. FE coordinates versus applied stress for a bar of FE-phase PZT 4.7 (SP14B #8) with flat, deep and shallow locations plotted separately

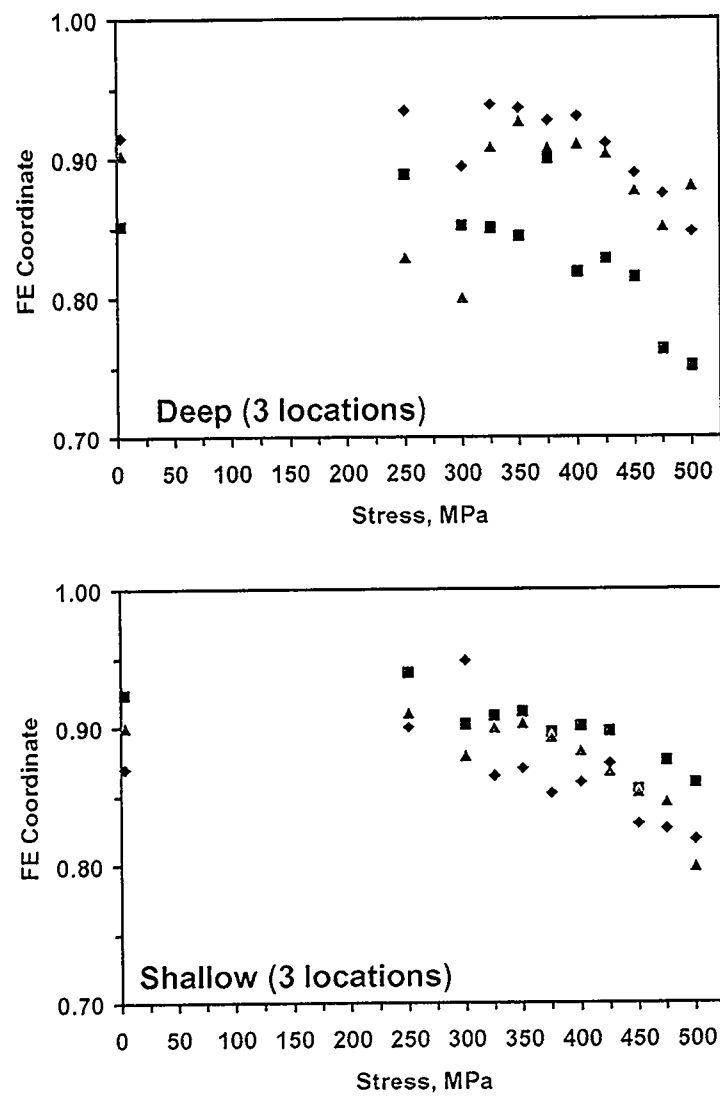


Figure 24. FE coordinates versus applied stress for a bar of FE-phase PZT 4.7 (SP14B #15) with deep and shallow locations plotted separately

Summary

An important conclusion from the Raman spectroscopic data is that, on the microscopic level, the FE-to-AFE transition is not progressive and uniform and does not occur simultaneously in all PZT grains as the uniaxial stress increases. Rather, the transformation initiates at different stresses and proceeds to different extents in different grains, not occurring at all in some grains stressed to 425 MPa. This inhomogeneity in the FE-to-AFE transformation can occur at dimensions of tens of micrometers or less. The variability in the response of different grains to macroscopically applied stress is believed to be due to local differences in grain size, shape or orientation (of domains) and local stress. In this regard we note that the stress at (or within a few micrometers of) the surface of a PZT bar, where the Raman measurements were obtained, is not necessarily the same as in its bulk, of which the strain gauge measurements are more representative. However, we also note that, given the porosity of these bars, a large percentage of the PZT grains will effectively be at a surface, be it external or internal. Effects such as increased stress at pores or, alternately, stress relief by expansion at pores will be felt at pores throughout the PZT bar. The presence of untransformed FE regions neighboring others which have been converted to the AFE phase has been suggested as contributing to anomalies observed in low-temperature PZT testing [Anderson, 1998].

Our standards for the FE coordinate calculation are Raman spectra of nominally phase pure FE PZT 4.4/4.7 (FE coordinate = 1.00) and AFE PZT 98/2 (FE coordinate = 0.00). As we noted earlier, the FE coordinate is not necessarily an absolute fraction or percentage of FE phase in the sampled region of the PZT bar, but it does provide a relative measure of changes in FE/AFE phase ratios. The largest uncertainty, besides the lack of spectra from intermediate FE/AFE phase compositions, is how similar the Raman spectra a PZT 4.4 or 4.7 composition, completely transformed to AFE phase by stress, is to the reference AFE spectrum from PZT 98/2. This issue could be resolved by measuring the Raman spectrum of PZT 4.4 and 4.7 materials as they are subjected to hydrostatic pressure sufficient to transform them completely to the AFE phase.

Even given these uncertainties in the interpretation of the Raman spectra, three general conclusions can be drawn from the FE coordinate plots. First, there is significant variability in the initial FE/AFE phase composition of the PZT grains. The first Raman spectrum for each bar was obtained at a few MPa, which is just enough stress to hold the bar firmly in the load frame. The FE coordinate values obtained from these initial spectra range from near 0.80 to just over 1.00. Second, at the maximum stresses (400 -500 MPa) achieved, the lowest FE coordinate is near 0.6, suggesting a less than complete transformation of FE bar compositions to the AFE phase. Third, larger applied stresses would probably drive the FE-to-AFE transformation further to completion, since the FE coordinates are on an approximately linear downward trend even at 500 MPa (Figures 20 and 24). Larger uniaxial stress might be achieved with bars of smaller cross section, assuming that we can avoid catastrophic failure of the bars.

Despite the fact that the strain gauges measure the macroscopic response of the PZT bars to uniaxial stress and the Raman spectra monitor the response of individual PZT grains at the microscopic scale, the data from the two types of measurements

have a general correlation. For the experiments involving all the PZT 4.4 bars (Figures 6-9) and one of the PZT 4.7 bars (Figure 13), the stress-strain plots show a distinct reversal in their lateral strain curves. This reversal is taken as an indication of significant FE-to-AFE transformation. The FE coordinate plots of the same bars (Figures 17-20 and 24) show distinct downward trends in the FE coordinate at nearly all the monitored locations at the highest applied stresses. In the FE coordinate plots (Figures 21-23) of those PZT 4.7 bars whose lateral strain plots (Figures 10-12) do not have a distinct reversal, the majority of the locations monitored do not show a significant downward trend in the FE coordinate at high stress.

In the stress-strain plots the departure of the volume strain from nonlinearly towards compression and the beginning of the reversal of the lateral strain towards compression are taken as indicators of the onset of the FE-to-AFE transition. The strain data indicates that this transition occurs near 150 MPa. In the FE coordinate plots the analogous indicator is the first sustained downward trend in the FE coordinate, which occurs between 200 and 300 MPa for the PZT 4.4 bars and at or above 300 MPa for the PZT 4.7 bars. Depoling data for PZT 4.7 compositions [Tuttle, 2000] indicates that the FE-to-AFE transition occurs between 250 and 350 MPa. It is probable that the strain measurements are indicating subtle structural adjustments in response to stress before they are substantial enough to significantly affect the polarization or the vibrational characteristics of the PZT materials.

Finally, we note that we have developed a capability for applying uniaxial stress to a material while simultaneously obtaining Raman spectra and strain measurements. This capability should have general application to materials in which the structural response to stress results in an observable change in their vibrational spectra.

Acknowledgements

We thank Jim Voigt for supplying the PZT materials and John Aidun for numerous useful discussions and support.

References

R. A Anderson, Electrical Breakdown, Permittivity and Polarization Kinetics of PZT 95/5. Sandia National Laboratories memorandum to Gordon Pike, January 5, 1998.

I. J. Fritz, Stress effects in two modified lead zirconate titanate ferroelectric ceramics, in J. Appl. Phys., vol. 50, pp. 5265-5271, 1979.

Galactic Industries software: GRAMS/32 v. 5.21, PLS/IQ v. 4.00.5000, 1999.

R. D. Hardy, Event Triggered Data Acquisition in the Rock Mechanics Laboratory, SAND93-0256, Sandia National Laboratories, Albuquerque, NM, 1993.

D. R. Tallant and R. L. Simpson, Raman Analysis of PZST Films #24, 25 and 28 (RAM97022.001), Sandia National Laboratories memorandum to Bruce Tuttle, October 24, 1996.

D. R. Tallant and R. L. Simpson, PZT Phase Transformation Project Feasibility, Sandia National Laboratories memorandum to D. Zeuch, July 3, 1997.

B. A. Tuttle, Initial results on effect of porosity on depoling pressure, Sandia National Laboratories internal e-mail to J. A. Voigt et al. January 24, 2000.

J. A Voigt, D. L. Sipola, K. G. Ewsuk, B. A. Tuttle, R. H. Moore, T. V. Montoya and M. A. Anderson, Solution Synthesis and Processing of PZT Materials for Neutron Generator Applications, SAND98-2750, Sandia National Laboratories, Albuquerque, NM, December, 1998.

D. H. Zeuch, S. T. Montgomery, D. J. Holcomb, J. M. Grazier and L. W. Carlson, Uniaxial Compression Experiments on PZT 95/5-2Nb Ceramic: Evidence for an Orientation-Dependent, 'Maximum Compressive Stress' Criterion for Onset of the FR1 \rightarrow AO Polymorphic Phase Transformation, SAND99-0077, Sandia National Laboratories, Albuquerque, NM, 1999.

D. H. Zeuch, S. T. Montgomery and D. J. Holcomb, Uniaxial compression experiments on lead zirconate titanate PZT 95/5-2Nb ceramic: evidence for an orientation-dependent, 'maximum compressive stress' criterion for onset of the ferroelectric to antiferroelectric polymorphic phase transformation, (to be published in the Journal of Materials Research).

DISTRIBUTION:

1	MS 0333	R. A. Anderson, 01846
1	MS 0513	A. D. Romig, 01000
1	MS 0515	J. D. Keck, 02561
1	MS 0521	S. T. Montgomery, 02567
1	MS 0751	J. M. Grazier, 06117
1	MS 0751	D. H. Zeuch, 06117
1	MS 1405	R. P. Goehner, 01822
1	MS 1405	B. A. Tuttle, 01846
1	MS 1405	W. R. Olson, 01846
1	MS 1411	R. L. Simpson, 01822
5	MS 1411	D. R. Tallant, 01822
1	MS 1411	J. A. Voigt, 01843
1	MS 1421	G. A. Samara, 01160
1	MS 1427	S. T. Picraux, 01100
1	MS 1435	A. K. Hays, 01800
1	MS 9018	Central Technical Files, 8940-2
2	MS 0899	Technical Library, 9616
1	MS 0612	Review & Approval Desk, 9612 For DOE/OSTI
1	MS 0188	LDRD, 4000